Physicochemical and rheological characterization of a novel hydrocolloid extracted from Althaea officinalis root

Shafagh Karimi [a], Babak Ghanbarzadeh [b,**], Leila Roufegarinejad [a], Pasquale M. Falcone [c,*]

[a] *Department of Food Science and Technology, Tabriz Branch, Islamic Azad University, Tabriz, Iran*
[b] *Department of Food Science and Technology, Faculty of Agriculture, University of Tabriz, P.O. Box 51666-16471, Tabriz, Iran*
[c] *University Polytechnical of Marche - Department of Agricultural, Food and Environmental Sciences, Brecce Bianche 10, 60131, Ancona, Italy*

ARTICLE INFO

ABSTRACT

Althaea officinalis L. root polysaccharide (AOP) was extracted, and its physicochemical and rheological properties were investigated. Gel permeation chromatography results showed that the molecular weight was 1560 kDa. High-performance liquid chromatography indicated that it was an acidic heteropolysaccharide consisting of five types of monosaccharides including galacturonic acid (40.2%), rhamnose (31.7%), glucose (13.68%), galactose (9.07%), and arabinose (5.35%). The intrinsic viscosity value for AOP in deionized water was 9.4 dl g^{-1}. The AOP solutions at different concentrations (0.5%, 1%, 2%, and 3% w/v), showed shear-thinning behavior, and the apparent viscosity decreased in the presence of different concentrations of NaCl and at different pHs. The frequency sweep test showed the AOP solutions at concentrations less than 0.5% and above 1% exhibited viscous and weak gel behavior, respectively. Since the hysteresis phenomenon was observed in the temperature sweep test of 2% AOP solution, it can be considered as a thermal irreversible gel during the heating and cooling process.

1. Introduction

One of the potential sources of plant polysaccharides is the root of *Althaea Officinalis* L. (AO). It belongs to the Malvaceae family and is commonly known as marshmallow (Pakrokh Ghavi, 2014). Traditionally, mucilage of marshmallow root and flower is used crudely in the treatment of cough, sore throat, gastrointestinal inflammation, anti-constipation, colds, gastritis, and other oral and nasal inflammations as well as skin disorders (Heydarirad, Choopani, Pasalar & Jafari, 2016; Park, Kim, Sathasivam, Chung, & Park, 2021). The root of this plant contains 5%–10% of water-soluble polysaccharides about 2% of flavonoids, phenolic acid, coumarin, starch, pectin, and tannin (Deters et al., 2010). Previous research has also shown that marshmallow root polysaccharides have antioxidant properties, antimicrobial and anticancer properties (Karimi, Ghanbarzadeh, Roufegarinejad, & Falcone, 2021; Pakrokh Ghavi, 2014; Hashemifesharaki, Xanthakis, Altintas, Guo & Gharibzahedi, 2020).

Polysaccharides can have various functional properties in different foods such as thickening, gelling, colloid stabilizing, emulsifying, film-forming, crystal growth suppressing, antistaling, fat replacing and fiber-prebiotic features. Since polysaccharides are usually high molecular weight macromolecules and have a high water absorption capacity, they are commonly used in food formulations as a thickening, gelling, or texture modifying agent which is accompanied by a change in their flow behavior (Li & Nie, 2015; Xu, Dong, Gong, Sun, & Li, 2015). The rheological behavior and viscosity of polysaccharides depend, largely, on various factors such as molecular weight, structural properties, concentration, environmental conditions (salt, sugar, and pH), and temperature. Thus, investigating the flow behavior of gum solutions in different conditions provides researchers with very valuable information, as it plays an important role in designing the production process, modeling, storage period, and sensory properties (Bourbon et al., 2010). The solution of the acidic fraction of marshmallow root gum at concentrations higher than 1% has a shear-thinning and a weak gel-like behavior (Karimi et al., 2021). On the other hand, the polysaccharide extracted from marshmallow flower at the concentrations between 0.5 and 5% showed pseudoplastic flow behavior and with increasing concentration from 2% to 5% at low temperature, a solid-like behavior was observed (Tabarsa, Anvari, Joyner, Behnam & Tabarsa, 2017). So far, no comprehensive research and detailed data are not available on the rheological properties of AO root polysaccharide (AOP). Thus, in this study, we extracted polysaccharides from AO root and after

---

precipitation with ethanol 96% was called AOP. The first some chemical composition, molecular weight, sugar composition, and intrinsic viscosity were analyzed; and the second the effect of concentration, salt, and pH on the steady and dynamic shear rheological properties of AOP solutions were investigated.

2. Materials and methods

2.1. Materials

Althaea Officinalis L. (AO) roots were harvested in Sanandaj, Iran (in Jun 2019). Ethanol 96% was prepared from Sahand Maragheh Company. Acetone, NaCl, HCl, NaOH, sulfuric acid, and methanol were purchased from Mojalal Company. The chloroform, phenol, *m-Hydroxydiphenyl*, glucose, D-galacturonic acid, potassium sulfate, sodium tetraborate, 1-phenyl-3-methyl-5-pyrazolone (PMP), trifluoroacetic acid (TFA), Folin reagent, sodium carbonate, Gallic acid, quercetin, aluminum chloride, potassium acetate, and sodium azide were purchased from Sigma-Aldrich Chemical Co. (USA).

2.2. Polysaccharide extraction from marshmallow root

The polysaccharide obtained from the AO root was extracted according to the method of Pakrokh Ghavi, (2014) with some modification. At first, the roots of the marshmallow were dried and after peeling, they became powder. Then, 100 g of root powder was mixed with 96% ethanol to separate pigments, fats, monosaccharides, and other impurities, and stirred for 2 h at 60 °C, and then it was maintained for 12 h at 4 °C. The roots were then filtered and dried. In the next step, the sample was mixed with distilled water in a ratio of 1–20 and kept in a water bath at 70 °C for 2 h and exposed to 4 °C for complete hydration for 24 h. The mucilage was separated using a thin linen cloth, then 96% ethanol in a ratio of 1: 3 was used to precipitate polysaccharides from the mucilage and kept in the refrigerator for 24 h. The mucilage precipitate was filtered and separated with a linen cloth. Then, for more purity and complete removal of impurities, it was washed twice with 96% ethanol and acetone. The samples were then re-dissolved in distilled water and after centrifugation, the solution part was separated. Finally, AO root polysaccharide (AOP) was dried in an oven at 45 °C for 18 h and stored at −18 °C.

2.3. Chemical composition

The determination of moisture content and ash content were determined according to A.O.A.C (2005) methods. The percentage content nitrogen was detected using CHNS analyzer (Costech, ECS 4010, CHNS–O Analyzer, Italy). The protein content was estimated by multiplying the nitrogen content (%) by 6.25. Total sugar was measured by the phenol-sulfuric acid method at the wavelength of 490 nm D-glucose as a standard (Dubois, Gilles, Hamilton, Rebers, & Smith, 1956). The amount of uronic acid was determined by the m-hydroxy diphenyl method and D-galacturonic acid was used as the standard (Blumenkrantz & Asboe-Hansen, 1974). To measure the amount of total phenol in AOP, the Folin–Ciocalteu assay method was used. The total phenolic content of the samples was calculated from the gallic acid standard curve, and the results were expressed as mg of gallic acid equivalents (mg GAE)/g of dried hydrocolloids. (Keshani-Dokht, Emam-Djomeh, Yarmand, & Fathi, 2018). The aluminum chloride colorimetric technique was used to measure total flavonoid content and the result was expressed as mg of quercetin equivalents (mg QE)/g of dry gum (Qin, Wang, Shan, Hou, & Ren, 2010). The extraction yield of polysaccharides was calculated by the following formula:

$$\text{Extraction yield } (\%) = (W_1/W_0) \times 100 \tag{1}$$

where W_1 and W_0 are the weights of crude polysaccharides and dried root OA, respectively.

2.4. Molecular weight determination test by GPC

To measure the average molecular weight of AOP, gel permeation chromatography (GPC) was used. 1 mg of the powder was dissolved in distilled water and after filtering (0.22 μm), 50 μl of the sample was injected into the device at 35 °C. 0.1 M NaNO3 at a rate of 0.5 ml/min was applied as the mobile phase, and dextran with different molecular weights was used as the standard. The specifications of the GPC machine were as follows: gel permeation chromatography machine (Shimadzu LC-20A, Japan); column with dimensions of 300 × 7.8 mm (Ultra hydrogel, Waters, USA) with RID detector (Shimadzu, Japan).

2.5. Determination of monosaccharide composition

Identifying AOP monosaccharide compounds was conducted by high-performance liquid chromatographic (HPLC). The polysaccharide derivation method was used by Phenyl-3-methyl-5-pyrazolone (PMP) reagent (Karimi et al., 2021). First, 5 mg of dry polysaccharide powder was mixed with 4 ml of trifluoroacetic acid (4 M) in a glass tube and hydrolyzed at 110 °C for 6 h. For derivation, 200 μl of the hydrolyzed sample was mixed with 200 μl of NaOH (0.3 M) and 200 μl of PMP methanolic solution (0.5 M). After stirring at 70 °C for 2 h, it was kept in the oven so that derivation reaction would be conducted. After cooling, the solution was neutralized by HCl (0.3 M) and 1 ml of chloroform (3 times) was added. The bottom layer of the solution was separated and after filtration (0.45 μm) was injected into the HPLC machine (Shimadzu, Japan). Meanwhile, the standard monosaccharides (galacturonic acid, glucose, rhamnose, arabinose, xylose, mannose and galactose) derived from 1-phenyl-3-methyl-5-pyrazolone were used as reference. The type of column was C18 (7.7 × 300 mm) (Agilent, USA) with a refractive index detector (RID). A mixture of 0.1 M phosphate buffer (pH 6.7) and acetonitrile in a ratio of 80:20 (v/v) was used as the mobile phase with a flow rate of 1.0 mL/min.

2.6. Intrinsic viscosity measurement

To measure the intrinsic viscosity [η], a Cannon-Fenske viscometer (Pyrex Fan, Iran) at 25 °C with a constant of 0.00336 mm^{2}s^{-1} was used. Four concentrations of AOP powder (0.02%, 0.04%, 0.06% and 0.08% w/v) were prepared in distilled water and kept at refrigerator temperature for 24 h. Then 10 ml of each of these solutions was placed inside the viscometer. After calculating the relative viscosity (Eq. (2)) and specific viscosity (Eq. (3)), the intrinsic viscosity was obtained by extrapolating the reduced or inherent viscosities to infinite dilution according to the Kraemer (Eq. (4)) and Huggins (Eq. (5)) equations:

$$\eta_{rel} = \frac{\eta}{\eta_0} \tag{2}$$

$$\eta_{sp} = \eta_{rel} - 1 \tag{3}$$

$$\eta_{inh} = \frac{\ln \eta_{rel}}{C} = [\eta] + K_K[\eta]^2 C \tag{4}$$

$$\eta_{red} = \frac{\eta_{sp}}{C} = [\eta] + K_H[\eta]^2 C \tag{5}$$

Where η_{rel} is relative viscosity, η_0 is solvent phase viscosity, η is dispersion phase viscosity, η_{inh} is inherent viscosity, η_{red} is reduced viscosity, η_{sp} is specific viscosity, C (g/dl) is the mass concentration of AOP, K_K indicates the Kraemer's constant, K_H shows the Huggins constant and [η] (dl.g^{-1}) is the intrinsic viscosity.

2.7. Rheological properties of AOP

Rheological properties of AOP solutions were performed by *Anton Paar rheometer* (GmBH, MCR301, Australia) equipped with concentric cylinder geometry with a diameter of 50 mm and a gap size of 0.206 mm.

2.7.1. Steady shear rheological analysis

2.7.1.1. Shear stress-shear rate relationship. To investigate the flow behavior of the AOP solutions, its different concentrations (0.5%, 1%, 2%, and 3%) were prepared in distilled water, and it was kept at refrigerator temperature for 24 h for complete hydration. To prevent microbial contamination, sodium azide (0.02% w/v) was added to each of the solutions. The Steady rheological properties of the gum solution were determined at the shear rate range of 0.01–100 s^{-1} at 25 °C.

Shear stress-shear rate data were fitted by Herschel–Bulkley (Eq. (6)) and Cross (Eq. (7)) models:

$$\sigma = k_H(\dot{\gamma})^{n_H} + \sigma_{0H} \qquad (6)$$

Where, σ: shear stress (Pa); $\dot{\gamma}$: shear rate (s^{-1}); k_H: consistency coefficient (Pa.s^n); n: flow behavior index (dimensionless); σ_{0H}: the yield stress (Pa).

$$\eta_a = \eta_\infty + \frac{(\eta_0 - \eta_\infty)}{1 + (\alpha_c\dot{\gamma})^m} \qquad (7)$$

η_a is apparent viscosity (Pa.s), η_∞ is the infinite- shear viscosity (Pa.s), η_0 is zero-shear viscosity (Pa.s), α_c is time constant, $\dot{\gamma}$ is the shear rate (0.01–100 s^{-1}), and m is a dimensionless exponent that captures the strength of the shear-thinning effect.

2.7.1.2. Effect of salt and pH on apparent viscosity. The effect of different concentrations of NaCl (0.1, 0.25, and 0.5 M) on the apparent viscosity of the solution of 2% (w/v) gum was evaluated (Li, Liao, Thakur, Zhang, & Wei, 2017). Also, after preparing a 2% solution of AOP at different pHs of 3.0, 5.0, 9.0, and 11.0, the relationship between shear stress and apparent viscosity was investigated. HCL and NaOH with a concentration of 0.1 M were used to adjust the pH of the solution. Changes in apparent viscosity were investigated at the shear rate range of 0.01–100 s^{-1} at 25 °C.

2.7.1.3. Time-dependent rheological behavior (Thixotropic properties). Thixotropic properties of different concentrations of the gum (0.5%, 1%, 2%, and 3% w/v) were determined according to the method of Wang, Yin, Huang, and Nie (2019); it includes three phases of increasing the shear rate from 0.01 s^{-1} to 80 s^{-1} in 160 s, rest for 5 s in s^{-1} 80 and decreasing the shear rate from 80 s^{-1} to 0.01 s^{-1} in 160 s at 25 °C. The area between the up-down curves was calculated using Rheoplus/32 software (version V3.40) and hysteresis area was determined. Moreover, the effect of different concentrations of NaCl (0.1, 0.25, and 0.5 M) and different pHs (3-5-9-11) on the solution of 2% w/v gum was also investigated.

2.7.2. Dynamic rheological properties (Oscillatory shear test)

2.7.2.1. Strain sweep test. The viscoelastic behavior of gum solutions was examined with concentrations of 0.5%, 1%, 2%, and 3% w/v at a constant frequency of 1 Hz, in the strain range of 0.1%–100%, at a temperature of 25 °C. A strain sweep test was also performed for a 2% solution of gum at different concentrations of NaCl (0.1, 0.25, and 0.5 M) and different pHs (3.0, 5.0, 7.0, 9.0, and 11.0). Parameters such as storage modulus (G′), loss tangent (tan δ), loss modulus (G″), and critical strain value (γ_L) were calculated.

2.7.2.2. Frequency sweep test. This test was conducted in a linear viscoelastic region (1% strain) at different concentrations of the gum (0.5%, 1%, 2%, and 3% w/v), in the angular frequency range of 0.1–100 Hz, at the temperature of 25 °C. In addition, the effect of different concentrations of NaCl (0.1, 0.25 and 0.5 M) and different pHs (3.0, 5.0, 7.0, 9.0, and 11.0) on G′ and G″ moduli in 2% polysaccharide solution was also investigated. The parameters such as G′, G″, and loss tangent (tan δ = G″/G′) were calculated.

2.7.2.3. Temperature sweep test. The temperature sweep test was conducted at a constant strain of 1% (linear viscoelastic region) and a frequency of 1 Hz on a 2% polysaccharide solution. The process was conducted in three phases: the first phase was to increase the temperature from 5 °C to 100 °C; the second phase was keeping (18 s) at 100 °C; third phase was cooling from 100 °C to 5 °C. The rate of temperature increase was 10 °C/min, and changes in G′ and G″ moduli during the heating and cooling phases were recorded.

3. Results and discussion

3.1. Physicochemical properties of AOP

According to the results shown in Table 1, yield, moisture, ash, and protein were 7.68%, 2.033%, 3.7%, and 6.75%, respectively. Moreover, according to the standard curve of glucose and galacturonic acid, the amount of total carbohydrate and uronic acid were 87.52% and 38.25%, respectively. Studies in previous research have also confirmed the presence of acidic groups in the structure of the gum of marshmallow root (Deters et al., 2010). Moreover, total phenolic compounds and total flavonoids in AOP were 4.53 mg GAE/g and 0.047 mg QE/g of the dry matter, respectively. The results of the GPC test have indicated that the average molecular weight of AOP was 1560 kDa, which was more than the molecular weight of polysaccharide obtained from the root of *Periploca laevigata* (557 kDa) and *Salvia macrosiphon* seeds (400 kDa) (Hajji et al., 2019; Razavi, Cui, Guo & Ding, 2014). Although polysaccharides obtained from Basil seed (2320 kDa) and Persian gum (2590–4740 kDa) have a higher molecular weight (Naji-Tabasi, Razavi & Mohebbi, 2016; Fadavi, Mohammadifar, Zargarran, Mortazavian, & Komeili, 2014a).

3.2. Monosaccharides composition

The type and composition of monosaccharides in the AOP structure were evaluated using HPLC and through retention time and mass data of standard sugars (Fig. 1a and b). According to the results, AOP was composed of five types of monosaccharides, which included galacturonic acid (GalA), rhamnose (Rha), glucose (Glc), galactose (Gal), and arabinose (Ara) with molar percentages of 40.2%, 31.7%, 13.68%, 9.07%, and 5.35% respectively (Table 1). The presence of uronic acid in the structure of AOP was also confirmed in the uronic test. Based on the results, it can be concluded that this gum is an acidic

Table 1
Some physicochemical properties of AOP.

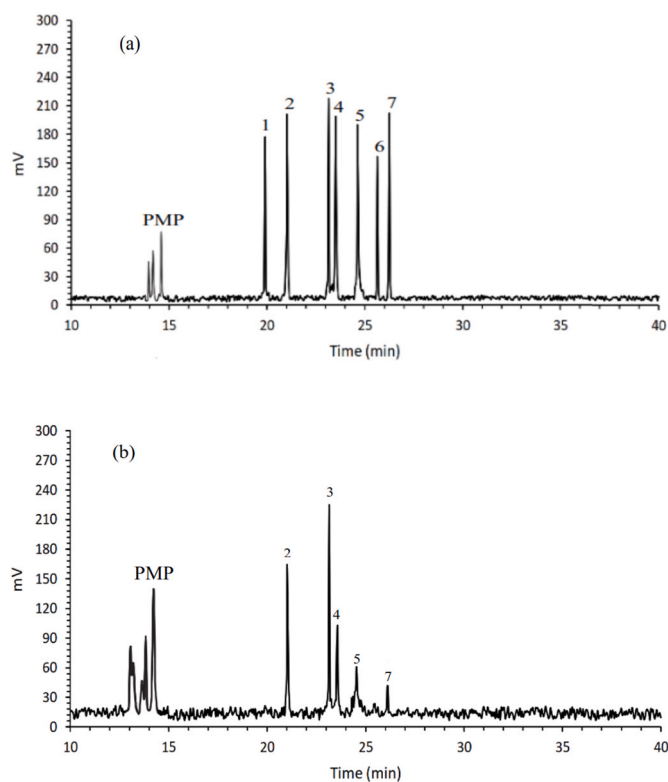| Parameters	AOP
Yield (%)	7.68 ± 0.02
Moisture (%)	2.03 ± 0.05
Ash (%)	3.7 ± 0.075
Total carbohydrate (%)	87.52 ± 1.12
Uronic acid (%)	38.25 ± 0.33
Protein (%)	6.75 ± 0.21
Total phenolic content (mg GAE/g)	4.53 ± 0.22
Total flavonoid content (mg QCE/g)	0.047 ± 0.018
MW (kDa)	1560 ± 0.3
GalA (%)	40.2
Rha (%)	31.7
Glc (%)	13.68
Gal (%)	9.07
Ara (%)	5.35

Fig. 1. (a) The HPLC chromatograms for standard monosaccharides, (b) sugar compositions of AOP. Peaks: (1) Man; (2) Rha; (3) GalA; (4) Glc; (5) Gal; (6) Xyl; (7) Ara.

heteropolysaccharide, in which rhamnose and galacturonic acid account for approximately 72% of the total monosaccharides. However, Hosseini-Parvar et al. (2010a) showed that the major monomers of a marshmallow root purified polysaccharide were Rha, Gal and Glc, followed by minor ones including, GalA, Ara and GlcA, that the amounts of sugars were different from the results obtained in this study. Also, the gum fractions obtained from *Althaea Officinalis* leaf was a neutral heteropolysaccharide and consisted of the monosaccharides of galactose, mannose, xylose, rhamnose, and glucose (Tahmouzi & Salek Nejat, 2020).

3.3. Intrinsic viscosity

The intrinsic viscosity ($[\eta]$) is a measure of the hydrodynamic volume occupied by the individual chains of a biopolymer. The intrinsic viscosity of AOP solution was estimated at 25 °C when the relative viscosity was in the range of 1.2–2 or the concentration of AOP was in the 0.02–0.08 (g/dl) range. As shown in Fig. 2a, the values of R^2 obtained in the Huggins and Kraemer equations were high ($R^2 > 0.92$), which indicates the high efficiency of these equations to determine $[\eta]$. The intrinsic viscosity of AOP was 9.4 dl g^{-1}, which was close to the one of *Salvia macrosiphon* seed gum (8.81–9.26 dl g^{-1}; 40 °C) (Razavi, Cui, Guo, & Ding, 2014). The intrinsic viscosity of biopolymer depends on molecular weight, structural configuration and stiffness, and solvent quality (Qian, Cui, Wu, & Goff, 2012). The previous studies have shown that the intrinsic viscosity of Guar, Tragacanth, and Persian gum were 11, 36.29–47.18, and 3.32–3.72 dl g^{-1}, respectively (Teimouri, Abbasi, & Sheikh, 2016; Wang, He, Guo, Zhao, & Tang, 2015). The configuration of many biopolymers in the solvent is a random coil. Molecular entanglement is determined by a dimensionless Berry number ($C[\eta]$), which is also called the coil-overlap parameter. In general, if the Berry number be below 1, the solution is in the dilute regime and no chain entanglement has occurred, and if it is between 1 and 10, the solution is in the
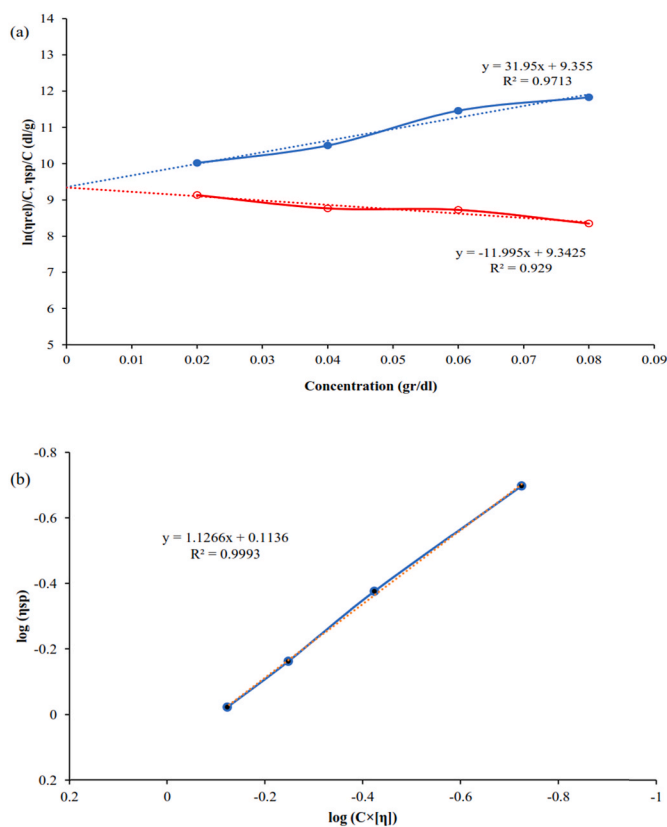

Fig. 2. (a) Huggins (filled symbols) and Kraemer (blank symbols) plot for AOP in deionized water, and (b) Master curve (log (ηsp)- log (C × $[\eta]$) for AOP in deionized water (25 °C).

semi-dilute regime (Behrouzian, Razavi, & Karazhiyan, 2014). The Berry number was 0.188–0.752, so it was in the dilute regime. To determine the dilute Newtonian domain and critical concentration, the master curve was drawn (Fig. 2b), which was obtained from the logarithm of the specific viscosity (log η_{sp}) vs the logarithm of the Berry number (log C $[\eta]$) (Naji-Tabasi, Razavi & Mohebbi, 2016). The slope of the master curve for the dilute domain is between 1 and 1.4 and for the semi-dilute domain is 2–5.1 (Piazza, Bertini, & Milany, 2010), which for the AOP solution was 1.126. The Huggins constant (K_H) is a measure of polymer-polymer interactions and shows the overall configuration of a polymer. The Huggins constant for flexible macromolecules with extended shapes in a good solvent is approximately 0.3–0.4, and values above 1 indicate polymer-polymer interactions and entanglement (Razmkhah, Razavi, & Mohammadifar, 2017). For the configuration of a random coil, there is a relationship between Huggins and Kraemer constants ($K_H + K_K = 0.5$). The K_H and K_K values of AOP were 0.361 and −0.135, respectively. $K_H + K_K$ value for the AOP was 0.496, indicating a flexible random coil structure. Since K_H was less than 0.5, the AOP solution was in a dilute regime and in a suitable solvent (Naji-Tabasi, Razavi & Mohebbi, 2016).

3.4. Steady shear rheological properties

3.4.1. Effect of AOP concentrations on the apparent viscosity

The apparent viscosity-shear rate relationship at different concentrations (0.5%, 1%, 2%, and 3%, at the shear rate of 0.01 s^{-1}) of AOP have been illustrated in Fig. 3a. As can be seen, by increasing concentration from 0.5% to 3% the apparent viscosity increased from 0.449 Pa s to 5.76 Pa s, respectively. In all samples, the apparent viscosity decreased by increasing the shear rate, indicating the shear thinning behavior. As can be seen from the slope of the curve, the pseudoplastic
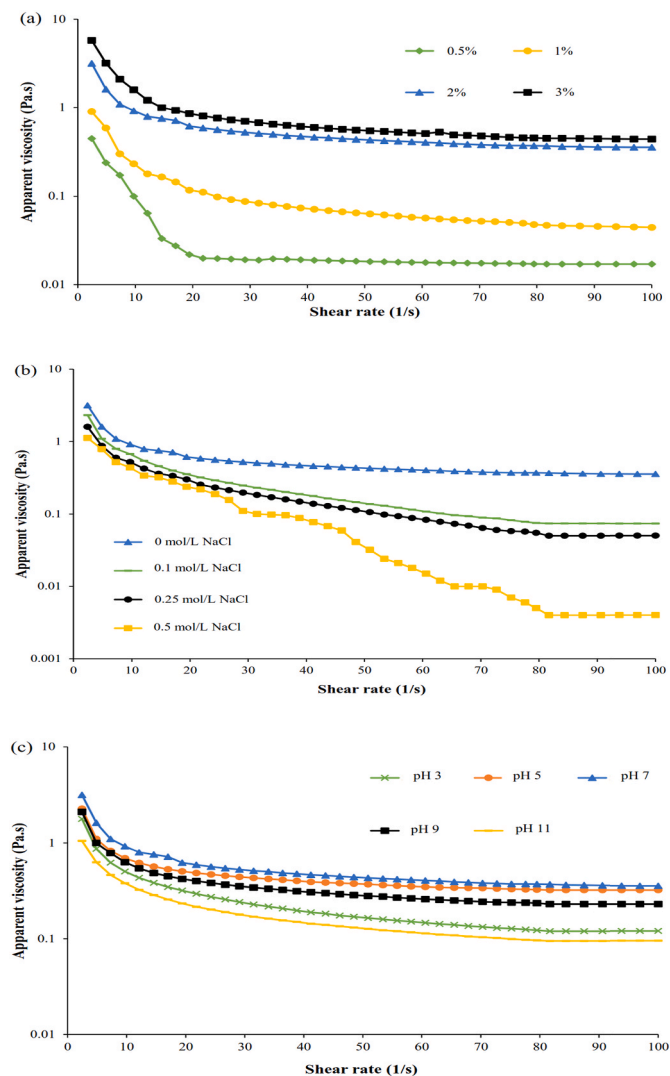
Fig. 3. (a) Steady shear flow curves of AOP solutions with different concentrations (0.5, 1, 2 and 3%), (b) effect of different concentrations of NaCl, and (c) different pHs on the apparent viscosity of AOP solution (2%, 25 °C).

behavior intensified at higher concentrations. For comparison, the apparent viscosity of some commercial gums such as welan, gellan, and xanthan at a concentration of 0.175% and at the shear rate of 0.1 s^{-1} were 7.665 Pa s, 2.776 Pa s, and 0.128 Pa s, respectively (Xu et al., 2015). As the polysaccharide concentration increases, strong interactions between the biopolymer chains are formed, and the free mobility of individual chains is limited leading to an increased polymerization, and this ultimately results in increased viscosity (Li et al., 2017). Most polysaccharide macromolecules indicate shear thinning behavior. At low shear rates, the polysaccharide chains have entanglement and dense structure. As the shear rate increases, the biopolymers chains are more oriented along with the flow, their entanglements are disrupted and water enclosed in them is released, resulting in decreasing of the apparent viscosity (Xu et al., 2015; Zeng et al., 2021).

The steady shear test data were fitted by different models including Herschel–Bulkley and Cross. According to the results (Table 2), when the concentration of polysaccharide solutions increased from 0.5% to 3%, the Herschel–Bulkley yield stress increased from 0.006 Pa to 8.85 Pa. The value of yield stress of gum solution is important when it is used as a binder to preserve the composition of the formulation and as a coating agent in some foods such as chocolate and ice cream (Zamani & Razavi, 2021). The values of yield stress in gums obtained from Basil seeds

Table 2
The parameters of shear rate – shear stress/apparent viscosity-based Herschel-Bulkley models for AOP solutions with different concentrations.

Model	0.5%	1%	2%	3%
Herschel – Bulkley				
σ_{0H} (Pa)	0.0065	0.7356	5.63	8.85
k_H (Pa.s^n)	0.0432	0.546	1.844	3.5
n_H	0.6161	0.483	0.3975	0.3454
R^2	0.999	0.9999	0.999	0.999
RMSE	0.0016	0.0171	0.1656	0.0557

(Hosseini-Parvar, Matia-Merino, Goh, Razavi, & Mortazavi, 2010a) and Chinese quince seed (Wang, Liu, et al., 2019) were 11.943 Pa (2%; 20 °C) and 36.77 Pa (2%; 25 °C), respectively. The amounts of consistency coefficient (k_H) increased from 0.0432 Pa.s^n to 3.5 Pa.s^n and the flow index (n) decreased from 0.6161 to 0.3454 as the concentration of AOP solutions increased from 0.5% to 3%. Therefore, pseudoplastic behavior is present in all concentrations, and the value of pseudo-plasticity degree increases as the concentration increases. Moreover, the R^2 value of Herschel–Bulkley model in all samples was above 0.99 and the RMSE value was low (0.0016–0557), indicating that this model is very suitable for predicting the rheological behavior of this gum.

The Cross model is another model describing the behavior of pseudoplastic fluids in which there are two important parameters of zero-shear viscosity (η_0), the infinite- shear viscosity (η_∞), and time constant (α_c) in its structure. As can be seen in Table 3, the zero-shear viscosity and infinite- shear viscosity increased from 0.32 to 0.001 Pa s at 0.5% concentration to 6.5–0.115 Pa s at 3% concentration. High viscosity at zero shear rate indicates the stiffness of biopolymer compounds, and infinite-shear rate viscosity shows the consistency of the product during processing such as pumping, mixing, and spraying (Razavi et al., 2014). At low shear rates (initial Newtonian plateau region), the disruption of entanglements by the imposed shear is balanced by the formation of new ones, so that no net change in entanglements occurs, and the viscosity shows a constant value (η_0). For higher shear rates, disruption predominates over the formation of new entanglements, molecules align in the direction of flow, and the apparent viscosity decreases with increasing shear rate, and shear-thinning behavior started. According to the results, the α_c value (relaxation time) increased from 1.12 s to 3.41 s, which is due to the increase in density and entanglement of chains. As the concentration of polysaccharides in the solution increases, the time increases for the biopolymer chains to interact with each other to form their original structure, after the stress has been removed and maintain its original structure (Huang, Zeng, Xiong, & Huang, 2016). Therefore, by increasing concentration, the mobility of individual chains is gradually limited, and the time required to form new structural forms (instead of destroyed structures) will increase. The shear rate corresponding to the transition from Newtonian to shear-thinning behavior moves to lower values, as the concentration increases (Bourbon et al., 2010). The parameter m is close to zero in Newtonian fluids and is close to 1 in highly pseudoplastic fluids (Bourbon et al., 2010). So that high viscosity degree (m 1) indicated strong shear thinning properties (Abbastabar, Azizi, Adnani, & Abbasi, 2014). By increasing the concentration from 0.5% to 3%, m value

Table 3
The parameters of cross model for AOP solutions with different concentrations.

Model	0.5%	1%	2%	3%
Cross model				
η_0 (Pa.s)	0.32	0.87	3.9	6.5
η_∞ (Pa.s)	0.001	0.025	0.079	0.115
a_c (s)	1.12	1.98	2.93	3.41
m	0.456	0.902	0.965	0.966
R^2	0.999	0.999	0.999	0.999
RMSE	0.0001	0.0004	0.0003	0.16

increased from 0.456 to 0.966, respectively. In all samples, the value was m < 1, indicating pseudoplastic behavior. Based on the results, it can be estimated that the cross model, owing to high R^2 (0.99) and low RMSE, can be a very good model to describe the rheological behavior in this study.

3.4.2. The effect of salt and pH on the apparent viscosity

The presence of salts effects on the functional properties of the polysaccharide solution, especially apparent viscosity. The effect of different concentrations of NaCl (0.1, 0.25, and 0.5 M) on the apparent viscosity of 2% AOP solution is reported in Fig. 3b. As can be seen, pseudoplastic behavior was observed at different NaCl concentrations and the apparent viscosity of the polysaccharide solutions decreased. According to the results obtained in Table 4, the apparent viscosity of the biopolymer solution at concentrations 0, 0.1, 0.25, and 0.5 M NaCl were 3.16, 2.32, 1.6, and 1.12 Pa s at the shear rate of 0.01 s^{-1}, respectively. The data suggested that AOP is sensitive to the presence of NaCl.The polysaccharide extracted in this study is an acidic polysaccharide in which the biopolymer chains are well dispersed in the solution, and increase the viscosity due to the high electrostatic repulsion force (Wang, Yin, et al., 2019). As the ionic strength increases, Na^+ ions bind to charged groups, reducing the electrostatic repulsion force, causing the chains to contract, increasing flexibility, reducing stiffness, and ultimately reducing the viscosity of the solution (Wang, Yin, et al., 2019). The changes in pH of biopolymer solutions can cause modification in the configuration of macromolecules, and subsequently change in the apparent viscosity. The apparent viscosity of gum solutions was investigated at five different pHs (Fig. 3c and Table 4) at the shear rate of 0.01 s^{-1}. All samples showed shear-thinning behavior, and the highest apparent viscosity of AOP (3.16 Pa s) was showed at pH 7.0. The apparent viscosity at pH 3.0, 5.0, 9.0, and 11.0 were 1.78, 2.27, 2.1, and 1.05 Pa s, respectively. The apparent viscosity was decreased at a lower or higher pH value (3.0 or 11.0) than pH 7.0. However, this decrease in alkaline pH was higher than in acidic conditions. Previous studies have indicated that acidic or alkaline environmental conditions degrade hydrogen bonds of polysaccharides, break down biopolymer chains, reduce molecular weight which finally leads to a decrease in the viscosity of the solution (Li et al., 2017).

3.4.3. Thixotropic properties

When thixotropic fluids are exposed to constant mechanical stress, their viscosity gradually decreases over time. When applying stress is paused in some of these fluids, they restore part of its structure and the viscosity returns partially to their original values (Qiao et al., 2016). In the shear stress-shear rate diagram of thixotropic fluids, the upward and downward curves do not match, and a loop called hysteresis is seen. The thixotropic degree is usually determined by calculating the area of the hysteresis loop, and the larger the area of hysteresis, the stronger the thixotropic property and the greater the dependence on time (Wang, Yin, et al., 2019). Fig. 4a shows the thixotropic behavior of different concentrations (0.5%, 1%, 2%, and 3% w/v) of AOP solutions at a shear rate of 1–80 s^{-1}. According to the results, in all samples, up-down curves

Table 4
Effects of different concentrations of NaCl and pH values on the apparent viscosity of AOP solution (2%, at the shear rate of 0.01 s^{-1}).

AOP solution (2%)	Apparent viscosity (Pa.s)
0 mol/L NaCl	3.16
0.1 mol/L NaCl	2.32
0.25 mol/L NaCl	1.6
0.5 M mol/L NaCl	1.12
pH 3.0	1.78
pH 5.0	2.27
pH 7.0	3.16
pH 9.0	2.1
pH 11.0	1.05

did not match, and hysteresis was observed in them, indicating thixotropic behavior. As the concentration of polysaccharide increased, the amount of relative hysteresis loop increased, showing a stronger thixotropic property. Thixotropic behavior can be attributed to rearrangement of the molecules in the direction of flow for decreasing of friction, opening of chain entanglements and disruption of interactions between macromolecule chains in three dimensional gel structure with increasing of shearing time at constant shear stress.

In another experiment, the effect of different concentrations of NaCl on the thixotropy of 2% AOP solution at 25 °C was investigated (Fig. 4b). The results indicated that by increasing the salt concentration, hysteresis area of the AOP solutions decreased in all samples. The thixotropic behavior of 2% AOP solution at different pHs was also investigated, and the results showed that both acidic and alkaline pH significantly reduced the hysteresis area and thixotropy (Fig. 4c).

The hysteresis loop is reported in Fig. 4d. As can be seen, the area values of hysteresis for the concentrations of 0.5%, 1%, 2%, and 3% w/v are 1.19, 7.97, 78.47, and 155.32 Pa s^{-1}, respectively, and it increased considerably when the AOP concentration increased. The amount of hysteresis of 2% AOP solution decreased from 78.47 Pa s^{-1} in the sample without salt to 28.05 Pa s^{-1} in the sample containing 0.5 M NaCl. Furthermore, the amount of hysteresis of 2% AOP solution decreased from 78.47 Pa s^{-1} in the sample with pH 7.0 to 2.98 Pa s^{-1} at pH 11.0. Polysaccharides was obtained from chia seeds at a concentration of 0.8% also showed thixotropic behavior, and hysteresis was observed in its curves (Goh et al., 2016).

3.5. Dynamic rheological properties

3.5.1. Strain-sweep oscillatory shear test

The strain-stress sweep test (amplitude test) is used to determine the linear viscoelastic (LVE) region and gel strength. In the LVE region (at low deformation), the storage (elastic) modulus (G′) and the loss (viscous) modulus (G″) are almost constant. It is important to determine this area before conducting the frequency sweep and temperature sweep tests, because dynamic tests are valuable when performed in a linear viscoelastic area. However, in the nonlinear region (at large deformation), the G′ and G″ moduli begin to decrease when the strain increases (Fadavi et al., 2014a). Moreover, using this test, strong gels can be distinguished from weak ones. As strong gels remain in the linear region more than weak gels, and the length of this region depends on the concentration (Wang, Liu, et al., 2019).
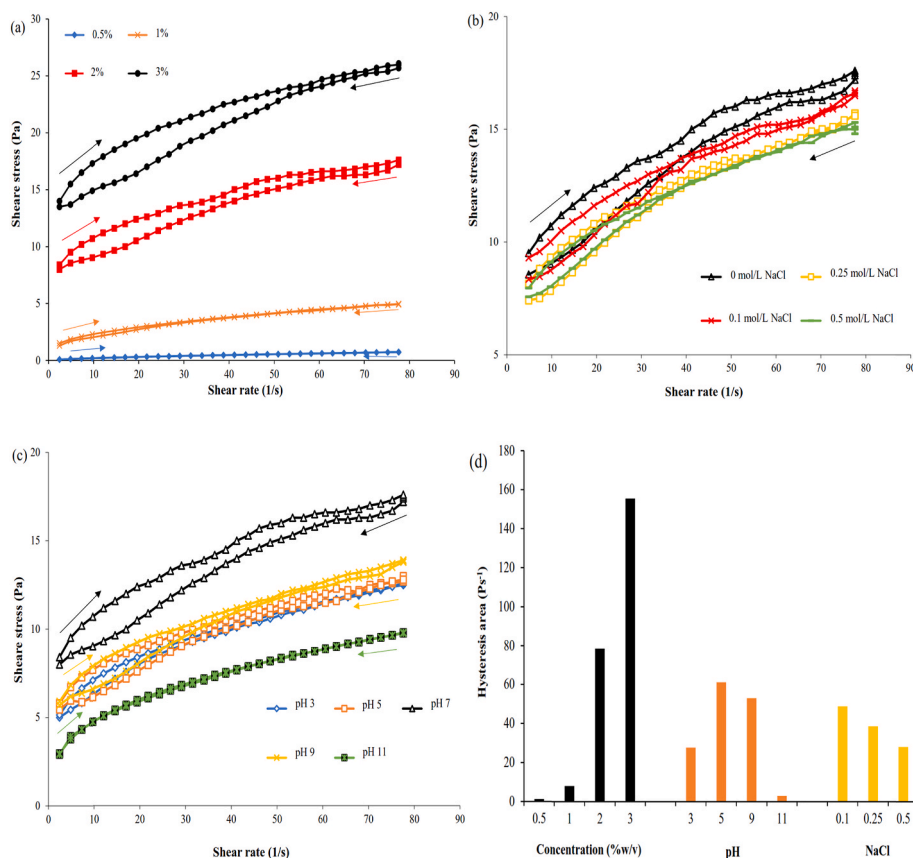
As shown in Fig. 5a, G′$_{LVE}$ was greater than G″$_{LVE}$ at concentrations of 1%, 2%, and 3%, indicating the behavior of a gel-like behavior, and it can be concluded that these dispersions can form a weak gel. However, at the concentration of 0.5%, the G′$_{LVE}$ was less than G″$_{LVE}$, and it showed the viscous behavior. Another parameter that evaluates the physical properties of gel systems is the loss tangent (tan δ), which was obtained from the ratio G″ to G′. In the elastic behavior tan δ < 1, and in the viscous behavior tan δ > 1 (Razmkhah, Razavi, & Mohammadifar, 2016). According to the results reported in Table 4, the amount of tan δ decreased as the concentration increased. In the 0.5% solution, the tan δ value was more than 1 (1.75), and it showed the viscous behavior, but in other samples tan δ values were less than 1 (0.234–0.445), indicating that the elastic behavior was dominant in the linear viscoelastic region.

The critical strain value (γ$_L$), which indicates the point at which the G′ modulus begins to decrease (LVE range), increased from 1.047% at the concentration of 0.5%–9.99% at the concentration of 3% (Fig. 5a). As a result, it can be estimated that by increasing concentration the resistance of solutions to deformation increases. It can be observed that by increasing concentration the resistance of the samples to flow increases, and the solid-like behavior becomes stronger. The addition of NaCl reduced the LVE and the critical strain value (Fig. 5b). However, in all samples G′ was higher than G″ without any intersection point, indicating the gel-like behavior. The tan δ values were in the range of 0.265–0.275, confirming the weak gel behavior in all samples. At higher

Fig. 4. (a) Hysteresis loops of flow curves for different concentration of AOP solutions (0.5, 1, 2, and 3%), (b) at different concentrations of NaCl, (c) at different pHs (2%, 25 °C), and (d) relative hysteresis area.

and less neutral pH, both the LVE and critical strain decreased (Fig. 5b), but the weak gel behavior (tan δ < 1) was observed in all samples (Table 5), indicating that the 2% solution of AOP had acceptable resistance over a wide range of pH. This gum has constituted from 40% uronic acid, so ions can change electrostatic interactions which lead to change in rheology and gelling properties. The values of the strain sweep parameters including G'_{LVE}, G'_{LVE}, tan δ_{LVE}, and γ_L have been reported in Table 5.

3.5.2. Frequency sweep oscillatory shear test

Frequency sweep test of biopolymer solutions is the most convenient oscillatory shear test and its results depend on various factors such as concentration, molecular weight, dispersion conditions (pH, ionic strength), structural properties (degree of branching, type of functional groups, and structure stiffness), and type of solvent (Fadavi et al., 2014a). Frequency sweep test for the AOP solutions was conducted at variable concentrations (0.5%, 1%, 2%, and 3% w/v) in the frequency range of 0.1–100 Hz, the constant strain of 1%, and at 25 °C (Fig. 6a). At the concentration of 0.5%, G'' (0.035 Pa) was higher than G' (0.021 Pa), and their values increased as frequency increased (high dependency on the frequency) without observing the crossover point. Moreover, the amount of tan δ was more than 1 (1.66), which indicated the behavior of a viscous dilute solution. However, at concentrations of 1%, 2%, and 3% G' was higher than G'', and they were partly dependent on frequency, indicating the behavior of a solid-like or weak gel behavior (Câmara et al., 2020). In real gels (strong gel) G' is greater than G'', but they are frequency-independent, and their diagram are seen as two parallel lines. As expected, as the concentration increases, the dependency of viscoelastic parameters on frequency (0.1–100 Hz) decreases, which can be attributed to the increase of interactions between the chains to form a complex structure that increases resistance to deformation (Zhou, Eid,

Xiong, Ren, & Ai, 2020).

Tan δ values for solutions containing 1%, 2% and 3% AOP were 0.753, 0.493 and 0.471, respectively. Since its value was less than 1, the elastic behavior was predominant, and it can be considered as a weak gel. Fig. 6b shows the frequency sweep analysis of 2% AOP solution at different concentrations of NaCl (0.1, 0.25, and 0.5 M). In all samples, the G' modulus was higher than the G'', and they showed the behavior of a weak gel. The G' values (ω = 1 Hz) for the solution containing 0.1, 0.25, and 0.5 M salt were equal to 4.58, 3.99, and 3.35 Pa, respectively which were lower than the values of the sample without salt (5.57 Pa). Moreover, tan δ (ω = 1 Hz) for solutions containing 0.1, 0.25 and 0.5 M of salt are equal to 0.519, −0.531, and 0.540, respectively. It can be concluded that AOP polysaccharide solution in the presence of different concentrations of NaCl showed good stability, and its gel-like behavior did not change. On the other hand, viscoelastic moduli showed little dependence on frequency. Fig. 6c shows the effect of different pHs (3.0, 5.0, 7.0, 9.0, and 11.0) on the viscoelastic parameters of 2% AOP solution. At both acidic and alkaline pHs in comparison to neutral conditions, the viscoelastic moduli values decreased, and the tan δ increased. In all samples except for the sample with pH 11.0, the G' modulus was higher than the G'' modulus, and the solid-like behavior were observed in them. However, the solution whit pH 11.0 exhibited a cross-over point; this point is defined as the point of gel formation. The G'' was primarily higher than the G' at low frequencies, and then they intersected as the frequency increased (Bai, Zhu, Wang, & Wang, 2020). This plot indicates that it is not good gelling agent in the condition (Milani, Ghanbarzadeh, & Maleki, 2012). The values of the parameters G', G'', and tan δ (ω = 1 Hz) are reported in Table 6.

3.5.3. Temperature-sweep oscillatory shear test

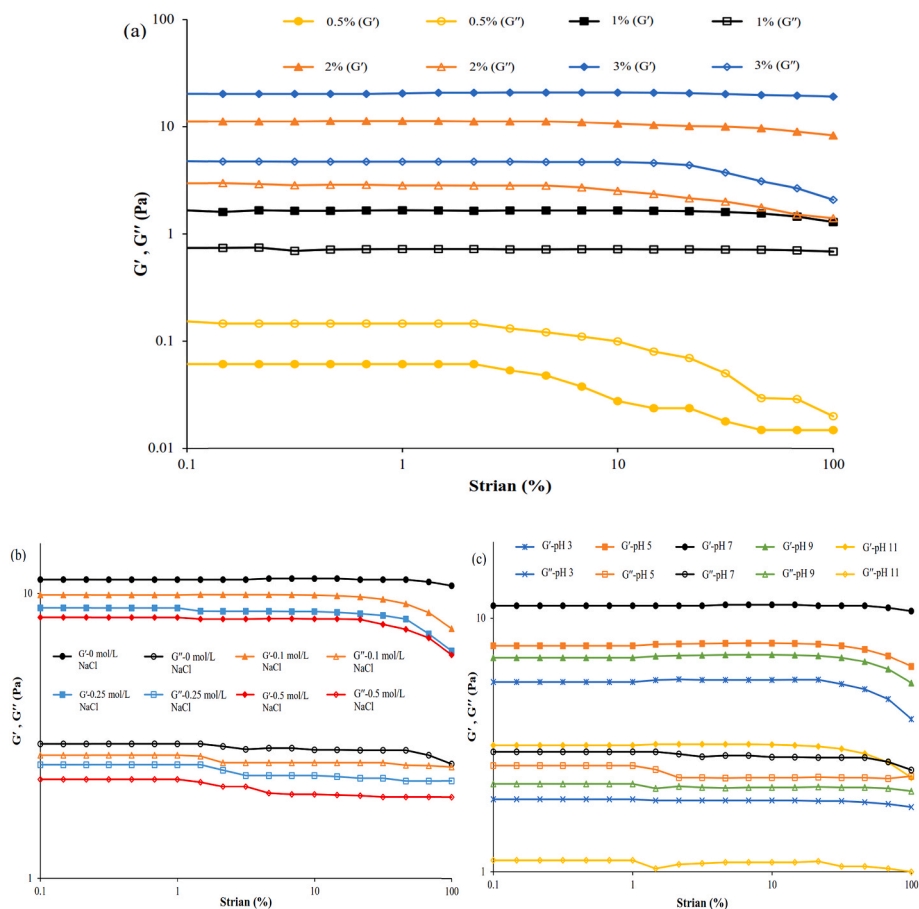In addition to concentration, the temperature is another factor that

Fig. 5. (a) Changes in G′ and G″ modulus in strain sweep test for AOP solutions with different concentrations (0.5, 1, 2, and 3%), (b) at different concentrations of NaCl, and (c) at different pHs (2%, $\omega = 1$ Hz, 25 °C).

Table 5
The strain sweep parameters of the AOP solutions with different concentrations, at different concentrations of NaCl, and at different pHs (2%, $\omega = 1$ Hz, 25 °C).

Concentration of AOP	G′ (Pa) $_{LVE}$	G″ (Pa) $_{LVE}$	Tanδ$_{LVE}$	γ_L (%)
0.5%	0.08	0.14	1.75	1.047
1%	1.66	0.74	0.445	3.16
2%	11.2	2.97	0.265	6.81
3%	20.3	4.77	0.234	9.99
Concentration of NaCl (mol/L)				
0.1	9.89	2.7	0.273	4.64
0.25	8.91	2.51	0.281	4.64
0.5	8.25	2.23	0.270	3.15
pH				
3.0	5.59	1.93	0.345	3.15
5.0	7.79	2.62	0.336	4.64
9.0	6.99	2.22	0.317	4.63
11.0	3.15	1.11	0.352	3.15

affects the formation and melting of gel. The results of the temperature sweep test, and its effect on viscoelastic functions are reported in Fig. 7. As the temperature increased from 5 °C to 90 °C, both G′ and G″ moduli decreased; the decrease in moduli is likely to be due to the breakdown of intermolecular interactions, the weakening of hydrogen bonds, and ultimately the increase in fluidity at high temperatures (Seo, Kang, Lee, Lee, & Chang, 2018). On the other hand, when temperature decreases, both moduli increase slightly without intersecting each other; this indicates the formation of a three-dimensional network between the molecules of the biopolymer structure at low temperatures (Lee, Jung, & Chang, 2020). Moreover, the G′ modulus was higher than G″ throughout the heating and cooling process, indicating heat stability of

weak gel structure and there is no phase transition (sol-gel) in them (Yuan, Li, Huang, & Fu, 2020). Since the phenomenon of hysteresis was observed during the heating and cooling process, this solution can be considered as thermally irreversible gels that which have not capable of returning to their original state. In one research conducted on basil seed gum, it has been reported that both the G′ and G″ moduli increased as the temperature increased, which attributed to the presence of hydrophobic groups, where the temperature strengthens the bond between them (Hosseini-Parvar, Matia-Merino, Goh, Razavi, & Mortazavi, 2010a). In other temperature sweep oscillatory tests on the polysaccharide solutions including h*igh methoxyl pectin from the pulp of tamarillo fruit* (Nascimento, Simas-Tosin, Iacomini, Gorin, & Cordeiro, 2016), the G′ and G″ moduli increased as the temperature decreased during the cooling process, and its cooling curves were higher than the heating ones, which could be attributed to the formation of new and stronger inter and intra-molecular interactions.

4. Conclusion

The rheological properties of a water-soluble acidic polysaccharide extracted from *Althaea officinalis* L. root (AOP) were evaluated. AOP had an intrinsic viscosity of 9.4 dl g^{-1} and average molecular weight of 1560 kDa, which could potentially give high viscosity, and be used as a thickening agent. The apparent viscosity and pseudo-plasticity of the AOP solutions increased with increasing concentration, and their values decreased with the addition of NaCl and in acidic and alkaline pH ranges. The AOP solutions showed thixotropic behavior, and increasing the concentration increased its thixotropic property. While in the presence of salt and acidic and alkaline pH ranges, the thixotropic behavior
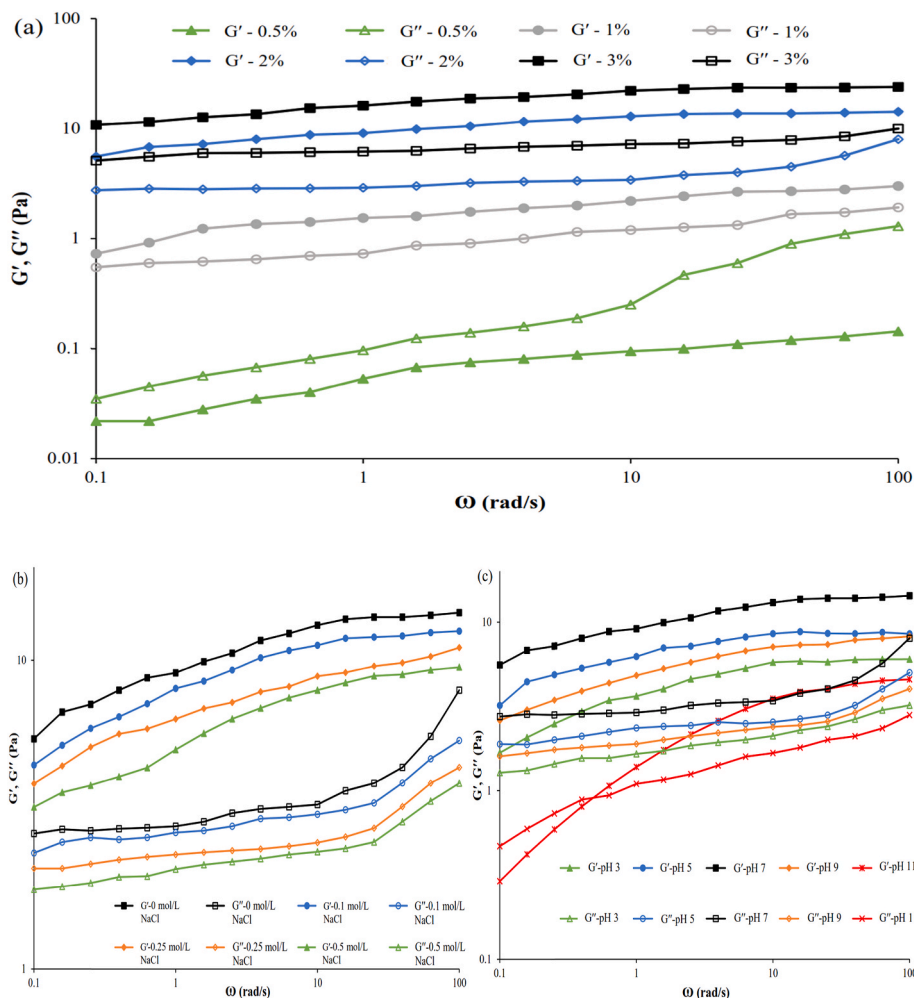
Fig. 6. (a) Changes in G′ and G″ moduli in frequency sweep test for AOP solutions with different concentrations (0.5, 1, 2, and 3%), (b) at different concentrations of NaCl, (c) at different pHs (2%, strain = 1%, 25 °C).

Table 6

The frequency sweep parameters of the AOP solutions with different concentrations, at different concentrations of NaCl, and at different pHs (2%, $\omega = 0.1$ Hz, strain = 1%, 25 °C).

Concentration of AOP	G′ (Pa)	G″ (Pa)	Tanδ
0.5%	0.021	0.035	1.66
1%	0.73	0.55	0.753
2%	5.57	2.75	0.493
3%	10.83	5.11	0.471
Concentration of NaCl (mol/L)			
0.1	4.58	2.38	0.519
0.25	3.99	2.12	0.531
0.5	3.35	1.81	0.540
pH			
3.0	1.68	1.28	0.761
5.0	3.2	1.89	0.590
9.0	2.61	1.60	0.613
11.0	0.291	0.469	1.611

Fig. 7. Changes in G′ and G″ moduli in temperature sweep test for AOP solution (2%, $\omega = 1$ Hz, strain = 1%, 25 °C).

decreased. The AOP dispersions exhibited typical viscoelastic behavior at concentrations of 1%, 2%, and 3%, but at a concentration of 0.5% showed a viscous-like behavior. According to the results of the temperature sweep test, the AOP solution (2%) formed thermally irreversible gels.
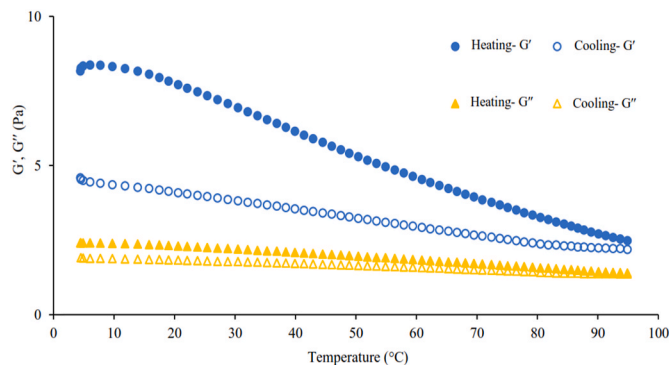
CRediT authorship contribution statement

Shafagh Karimi: Investigation, Writing – original draft. **Babak Ghanbarzadeh:** Supervision, Writing – review & editing. **Leila Roufegarinejad:** Adviser. **Pasquale M. Falcone:** Reviewing, Data curation, Validation.

Declaration of competing interest

The authors declare that they have no known competing financial interests or personal relationships that could have appeared to influence the work reported in this paper.

Data availability

Data will be made available on request.

Acknowledgments

References

Abbastabar, B., Azizi, M. H., Adnani, A., & Abbasi, S. (2014). Determining and modeling rheological characteristics of quince seed gum. *Food Hydrocolloids, 43*, 259–264.

Bai, L., Zhu, P., Wang, W., & Wang, M. (2020). The influence of extraction pH on the chemical compositions, macromolecular characteristics, and rheological properties of polysaccharide : The case of okra polysaccharide. *Food Hydrocolloids, 102*, Article 105586. https://doi.org/10.1016/j.foodhyd.2019.105586

Behrouzian, F., Razavi, S. M. A., & Karazhiyan, H. (2014). Intrinsic viscosity of cress (*Lepidium sativum*) seed gum: Effect of salts and sugars. *Food Hydrocolloids, 35*, 100–105. https://doi.org/10.1016/j.foodhyd.2013.04.019

Blumenkrantz, N., & Asboe-Hansen, G. (1974). An automated quantitative assay for uronic acids. *Biochemical Medicine, 11*(1), 60–66. https://doi.org/10.1016/0006-2944(74)90095-7

Bourbon, A. I., Pinheiro, A. C., Ribeiro, C., Miranda, C., Maia, J. M., Teixeira, J. A., et al. (2010). Food Hydrocolloids Characterization of galactomannans extracted from seeds of *Gleditsia triacanthos* and *Sophora japonica* through shear and extensional rheology : Comparison with guar gum and locust bean gum. *Food Hydrocolloids, 24*, 184–192. https://doi.org/10.1016/j.foodhyd.2009.09.004

Câmara, A. K. F. I., Okuro, P. K., Cunha, R. L. D., Herrero, A. M., Ruiz-Capillas, C., & Pollonio, M. A. R. (2020). Chia (Salvia hispanica L.) mucilage as a new fat substitute in emulsified meat products: Technological, physicochemical, and rheological characterization. *LWT - Food Science and Technology, 125*, Article 109193. https://doi.org/10.1016/j.lwt.2020.109193

Deters, A., Zippel, J., Hellenbrand, N., Pappai, D., Possemeyer, C., & Hensel, A. (2010). Cytoprotective effects of aqueous extracts from marshmallow roots (*Althaea officinalis* L.). *Journal of Ethnopharmacology, 127*(S 01), 62–69. https://doi.org/10.1055/s-0032-1313246

Dubois, M., Gilles, K. A., Hamilton, J. K., Rebers, P. A., & Smith, F. (1956). Colorimetric method for determination of sugars and related substances. *Analytical Chemistry, 28*(3), 350–356. https://doi.org/10.1021/ac60111a017

Fadavi, G., Mohammadifar, M. A., Zargarran, A., Mortazavian, A. M., & Komeili, R. (2014a). Composition and physicochemical properties of Zedo gum exudates from *Amygdalus scoparia*. *Carbohydrate Polymers, 101*(1), 1074–1080. https://doi.org/10.1016/j.carbpol.2013.09.095

Goh, K. K. T., Matia-Merino, L., Chiang, J. H., Quek, R., Soh, S. J. B., & Lentle, R. G. (2016). The physico-chemical properties of chia seed polysaccharide and its microgel dispersion rheology. *Carbohydrate Polymers, 149*, 297–307. https://doi.org/10.1016/j.carbpol.2016.04.126

Hajji, M., Hamdi, M., Sellimi, S., Ksouda, G., Laouer, H., Li, S., et al. (2019). Structural characterization, antioxidant and antibacterial activities of a novel polysaccharide from *Periploca laevigata* root barks. *Carbohydrate Polymers, 206*, 380–388. https://doi.org/10.1016/j.carbpol.2018.11.020

Heydarirad, G., Choopani1, R., Pasalar, M., & Jafari, J. M. (2016). Medical mucilage used in traditional Persian medicine practice. *Iranian Journal of Medical Sciences, 41*(3), Article PMC5103549.

Hosseini-Parvar, S. H., Matia-Merino, L., Goh, K. K. T., Razavi, S. M. A., & Mortazavi, S. A. (2010a). Steady shear flow behavior of gum extracted from *Ocimum basilicum* L. seed: Effect of concentration and temperature. *Journal of Food Engineering, 101*(3), 236–243. https://doi.org/10.1016/j.jfoodeng.2010.06.025

Huang, J., Zeng, S., Xiong, S., & Huang, Q. (2016). Steady , dynamic , and creep-recovery rheological properties of myofibrillar protein from grass carp muscle. *Food Hydrocolloids, 61*, 48–56. https://doi.org/10.1016/j.foodhyd.2016.04.043

Karimi, S., Ghanbarzadeh, B., Roufegarinejad, L., & Falcone, P. M. (2021). Polysaccharide extracted from *Althaea officinalis* L. root: New studies of structural, rheological and antioxidant properties. *Carbohydrate Research, 510*, Article 108438. https://doi.org/10.1016/j.carres.2021.108438

Keshani-Dokht, S., Emam-Djomeh, Z., Yarmand, M. S., & Fathi, M. (2018). Extraction, chemical composition, rheological behavior, antioxidant activity and functional properties of *Cordia myxa* mucilage. *International Journal of Biological Macromolecules, 118*, 485–493. https://doi.org/10.1016/j.ijbiomac.2018.06.069

Lee, Y. K., Jung, S. K., & Chang, Y. H. (2020). Rheological properties of a neutral polysaccharide extracted from maca (*Lepidium meyenii* Walp.) roots with prebiotic and anti-inflammatory activities. *International Journal of Biological Macromolecules, 152*, 757–765. https://doi.org/10.1016/j.ijbiomac.2020.02.307

Li, L., Liao, B., Thakur, K., Zhang, J., & Wei, Z. (2017). The rheological behavior of polysaccharides sequential extracted from *Polygonatum cyrtonema* Hua. *International Journal of Biological Macromolecules, 109*, 761–771. https://doi.org/10.1016/j.ijbiomac.2017.11.063

Li, J. M., & Nie, S. P. (2015). The functional and nutritional aspects of hydrocolloids in foods. *Food Hydrocolloids, 53*, 46–61. https://doi.org/10.1016/j.foodhyd.2015.01.035

Milani, J., Ghanbarzadeh, B., & Maleki, G. (2012). Rheological properties of anghouzeh gum. *International Journal of Food Engineering, 8*(3). https://doi.org/10.1515/1556-3758.2071

Naji-Tabasi, S., Razavi, S. M. A., Mohebbi, M., & Malaekeh-Nikouei, B. (2016). New studies on basil (*Ocimum bacilicum* L.) seed gum: Part I e fractionation, physicochemical and surface activity characterization. *Food Hydrocolloids, 52*, 350–358. https://doi.org/10.1016/j.carbpol.2016.04.088

Nascimento, G. E. D., Simas-Tosin, F. F., Iacomini, M., Gorin, P. A. J., & Cordeiro, L. M. C. (2016). Rheological behavior of high methoxyl pectin from the pulp of tamarillo fruit (*Solanum betaceum*). *Carbohydrate Polymers, 139*, 125–130. https://doi.org/10.1016/j.carbpol.2015.11.067

Pakrokh Ghavi, P. (2014). The extraction process optimization of antioxidant polysaccharides from Marshmallow (*Althaea officinalis* L.) roots. *International Journal of Biological Macromolecules, 75*, 51–57. https://doi.org/10.1016/j.ijbiomac.2014.11.047

Park, Y. J., Kim, N. S., Sathasivam, R., Chung, Y. S., & Park, S. U. (2021). Impact of copper treatment on phenylpropanoid biosynthesis in adventitious root culture of *Althaea officinalis* L. *Preparative Biochemistry & Biotechnology, 52*(3), 283–291. https://doi.org/10.1080/10826068.2021.1934697

Piazza, L., Bertini, S., & Milany, J. (2010). Extraction and structural characterization of the polysaccharide fraction of *Launaea acanthodes* gum. *Carbohydrate Polymers, 79*(2), 449–454. https://doi.org/10.1016/j.carbpol.2009.08.041

Qian, K. Y., Cui, S. W., Wu, Y., & Goff, H. D. (2012). Flaxseed gum from flaxseed hulls: Extraction, fractionation, and characterization. *Food Hydrocolloids, 28*(2), 275–283. https://doi.org/10.1016/j.foodhyd.2011.12.019

Qiao, L., Li, Y., Chi, Y., Ji, Y., Gao, Y., Hwang, H., et al. (2016). Rheological properties, gelling behavior and texture characteristics of polysaccharide from *Enteromorpha prolifera*. *Carbohydrate Polymers, 136*, 1307–1314. https://doi.org/10.1016/j.carbpol.2015.10.030

Qin, P., Wang, Q., Shan, F., Hou, Z., & Ren, G. (2010). Nutritional composition and flavonoids content of flour from different buckwheat cultivars. *International Journal of Food Science and Technology, 45*, 951–958. https://doi.org/10.1111/j.1365-2621.2010.02231.x, 2010.

Razavi, S. M. A., Cui, S. W., Guo, Q., & Ding, H. (2014). Some physicochemical properties of sage (*Salvia macrosiphon*) seed gum. *Food Hydrocolloids, 35*, 453–462. https://doi.org/10.1016/j.foodhyd.2013.06.022

Razmkhah, S., Razavi, S. M. A., & Mohammadifar, M. A. (2016). Purification of cress seed (*Lepidium sativum*) gum: A comprehensive rheological study. *Food Hydrocolloids, 61*, 358–368. https://doi.org/10.1016/j.foodhyd.2016.05.035

Razmkhah, S., Razavi, S. M. A., & Mohammadifar, M. A. (2017). Dilute solution, flow behavior, thixotropy and viscoelastic characterization of cress seed (*Lepidium sativum*) gum fractions. *Food Hydrocolloids, 63*, 404–413. https://doi.org/10.1016/j.foodhyd.2016.09.030

Seo, S. Y., Kang, Y. R., Lee, Y. K., Lee, J. H., & Chang, Y. H. (2018). Physicochemical, molecular, emulsifying and rheological characterizations of sage (*Salvia splendens*) seed gum. *International Journal of Biological Macromolecules, 115*, 1174–1182. https://doi.org/10.1016/j.ijbiomac.2018.04.173

Tabarsa, M., Anvari, M., Joyner, Melito, H, S., Behnam, S., et al. (2017). Rheological behavior and antioxidant activity of a highly acidic gum from *Althaea officinalis* flower. *Food Hydrocolloids, 69*, 432–439. https://doi.org/10.1016/j.foodhyd.2017.02.009

Tahmouzi, S., & Salek Nejat, M. R. (2020). New infertility therapy effects of polysaccharides from *Althaea officinalis* leaf with emphasis on characterization, antioxidant and anti-pathogenic activity. *International Journal of Biological Macromolecules, 145*, 777–787. https://doi.org/10.1016/j.ijbiomac.2019.12.224

Teimouri, S., Abbasi, S., & Sheikh, N. (2016). Effects of gamma irradiation on some physicochemical and rheological properties of Persian gum and gum tragacanth. *Food Hydrocolloids, 59*, 9–16. https://doi.org/10.1016/j.foodhyd.2015.12.010

Wang, S., He, L., Guo, J., Zhao, J., & Tang, H. (2015). Intrinsic viscosity and rheological properties of natural and substituted guar gums in seawater. *International Journal of Biological Macromolecules, 76*, 262–268. https://doi.org/10.1016/j.ijbiomac.2015.03.002

Wang, L., Liu, H. M., Zhu, C. Y., Xie, A. J., Ma, B. J., & Zhang, P. Z. (2019). Chinese quince seed gum: Flow behaviour, thixotropy and viscoelasticity. *Carbohydrate Polymers, 209*, 230–238. https://doi.org/10.1016/j.carbpol.2018.12.101

Wang, Y., Yin, J., Huang, X., & Nie, S. (2019). Structural characteristics and rheological properties of high viscous glucan from fruit body of *Dictyophora rubrovolvata*. *Food Hydrocolloids, 101*, Article 105514. https://doi.org/10.1016/j.foodhyd.2019.105514

Xu, L., Dong, M., Gong, H., Sun, M., & Li, Y. (2015). Effects of inorganic cations on the rheology of aqueous welan , xanthan , gellan solutions and their mixtures. *Carbohydrate Polymers, 121*, 147–154. https://doi.org/10.1016/j.carbpol.2014.12.030

Yuan, D., Li, C., Huang, Q., & Fu, X. (2020). Ultrasonic degradation effects on the physicochemical , rheological and antioxidant properties of polysaccharide from *Sargassum pallidum*. *Carbohydrate Polymers, 239*, Article 116230. https://doi.org/10.1016/j.carbpol.2020.116230

Zamani, Z., & Razavi, S. M. A. (2021). Physicochemical, rheological and functional properties of Nettle seed (*Urtica pilulifera*) gum. *Food Hydrocolloids, 112*, Article 106304. https://doi.org/10.1016/j.foodhyd.2020.106304

Zeng, Q., Zhang, L., Liao, W., Liu, J., Yuan, F., & Gao, Y. (2021). Effect of xanthan gum co-extruded with OSA starch on its solubility and rheological properties. *LWT - Food Science and Technology, 147*, Article 111588. https://doi.org/10.1016/j.lwt.2021.111588

Zhou, P., Eid, M., Xiong, W., Ren, C., & Ai, T. (2020). Comparative study between cold and hot water extracted polysaccharides from *Plantago ovata* seed husk by using rheological methods. *Food Hydrocolloids, 101*, Article 105465. https://doi.org/10.1016/j.foodhyd.2019.105465